ARTICLE

Detection of RadioCarbon Dioxide with Double-Resonance Absorption Spectroscopy

Yan-dong Tan[a], Cun-feng Cheng[b], Dong Sheng[a,b], Shui-Ming Hu[b*]

a. Department of Precision Machinery and Precision Instrumentation, University of Science and Technology of China, Hefei 230026, China
b. Hefei National Laboratory for Physical Sciences at the Microscale, University of Science and Technology of China, Hefei 230026 China

(Dated: Received on March 15, 2021; Accepted on April 12, 2021)

Fast and accurate quantitative detection of $^{14}CO_2$ has important applications in many fields. The optical detection method based on the sensitive cavity ring-down spectroscopy technology has great potential. But currently it has difficulties of insufficient sensitivity and susceptibility to absorption of other isotopes/impurity molecules. We propose a stepped double-resonance spectroscopy method to excite $^{14}CO_2$ molecules to an intermediate vibrationally excited state, and use cavity ring-down spectroscopy to probe them. The two-photon process significantly improves the selectivity of detection. We derived the quantitative measurement capability of double-resonance absorption spectroscopy. The simulation results show that the double-resonance spectroscopy measurement is Doppler-free, thereby reducing the effect of other molecular absorption. It is expected that this method can achieve high-selectivity detection of $^{14}CO_2$ at the sub-ppt level.

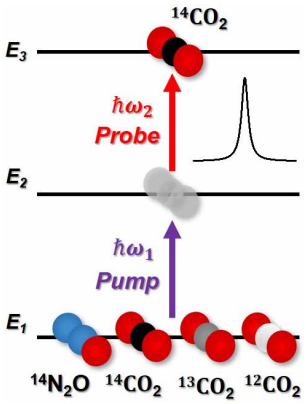

Key words: Double-resonance, Radiocarbon, Cavity ring-down spectroscopy

I. INTRODUCTION

^{14}C has a half-life of 5730 years [1], and it is the only radiocarbon isotope in nature. ^{14}C is mainly produced by the interaction of cosmic rays and nitrogen in the earth's atmosphere. Its isotopic abundance in the earth's biosphere is 1.176×10^{-12} [2]. ^{14}C in the biosphere mainly exists in the form of $^{14}CO_2$ in the gas phase, which diffuses through the global biological carbon cycle, and its concentration keeps almost constant. Its detection is widely used in fields such as dating and tracing [3, 4]. However, because of the low natural abundance of $^{14}CO_2$, its detection requires extremely high sensitivity and selectivity.

Accelerator mass spectrometry (AMS) is the most popular method for quantitative detection of ^{14}C at present, which greatly improves the sensitivity (10^{-15}) and reliability (error less than 1%) in the trace isotope analysis of ^{14}C [5]. Since Ruff *et al.* developed a mini radiocarbon dating system (MICADAS) for ^{14}C isotope dating, the sample type has been changed from solid carbon to gaseous CO_2 and the required sample size has been reduced from 1 mg solid carbon to less than 100 μg, which greatly promotes the application of AMS in various fields [6]. However, even for the small scale MICADAS, it costs millions of dollars, which limits the prospect of AMS to wide applications, such as atmospheric carbon cycle monitoring and drug development [7]. In addition, recent studies have found that the simultaneous measurement of concentration ratios of $^{14}CO_2$ and ^{14}CO in the atmosphere is very important for understanding the atmospheric carbon cycle [8, 9]. The AMS method needs to convert ^{14}CO into $^{14}CO_2$,

*Author to whom correspondence should be addressed. E-mail: smhu@ustc.edu.cn

DOI:10.1063/1674-0068/cjcp2103045

and obtain the ^{14}CO concentration indirectly by subtracting original $^{14}CO_2$ in the sample, which increases the measurement difficulty [10].

The optical method of molecular detection has a wide range of applications in climate change research, industrial pollution monitoring, and drug metabolism and archaeology [2, 11]. In recent years, due to the advancement of infrared lasers and coating technology, ultra-sensitive spectroscopy methods based on molecular vibration transitions have been rapidly developed [2] and the molecular detection has reached a sensitivity of one part per trillion (ppt) [12] or even better. Detection of trace gas and isotopes has attracted more and more interests.

In the last decades, infrared laser spectroscopy has been realized as a fast-developing method for isotopic quantitative measurement. Reid *et al.* first proposed to use infrared laser spectroscopy to realize radiocarbon isotope dating [13]. Since the progress of mid-infrared quantum cascade lasers (QCL) and mid-infrared coating technology, highly sensitive cavity-enhanced mid-infrared spectroscopy has been developed rapidly [14–17]. Mid-infrared laser ($400-4000$ cm^{-1}) has great advantages for trace gas detection since fundamental bands of molecules are mostly in this region, which are usually stronger than the overtones by $1-2$ or even more orders of magnitude [18]. On the other hand, cavity ring-down spectroscopy (CRDS) is a cavity-enhanced technique that obtains the absolute absorption coefficient of the sample by measuring the ring-down time of the light emitted from the cavity. It is not affected by laser power fluctuations, and thanks to the use of high-finesse resonant cavity, its sensitivity (minimum detectable absorption coefficient) can reach the level of 10^{-9} to 10^{-12} cm^{-1} [2]. Researchers from the Italian National Institute of Optics (INO) [19] and NIST of the United States [20] respectively demonstrated CRDS measurements of natural CO_2 samples at low temperatures, and $^{14}CO_2$ concentrations below the natural abundance were determined. Compared with the AMS method, although the sensitivity of laser spectroscopy is lower so far, it has advantages in terms of cost, mobility, and measurement speed. Further more, in order to accurately determine the source ratio of fossil fuel to biomass fuel in a target sample, it is necessary to measure the abundance ratio of ^{14}C to ^{13}C in the sample. At present the combined method of AMS and isotope ratio mass spectrometry (IRMS) has been used to measure the abundance of ^{14}C and ^{13}C, respectively, which has increased the difficulty for the practical application of source assessment of carbon emission. The laser spectroscopy method has a large dynamic range that in principle can measure ^{14}C, ^{13}C and other isotopes at the same time. In some applications that do not require high accuracy and sensitivity, such as biomedical surveying and earth science research, it is expected that the optical method has a wide range of applications [21].

Although the cavity-enhanced spectroscopy technology has achieved high sensitivity in measurements, the single-photon absorption method for detecting $^{14}CO_2$ requires improvements in both sensitivity and selectivity. The measurement signal is susceptible to the absorption of nitrogen oxides and other isotopes of carbon dioxide in the sample, which has become a bottleneck for the further development of optical measurement of $^{14}CO_2$. We propose to use stepped double-resonance CRDS to measure $^{14}CO_2$. The selective pumping and detection of double-resonance technology can effectively eliminate the interference due to absorption of other molecules in the single-photon absorption spectroscopy method. Combined with the high sensitivity characteristics of the CRDS technology, it allows for $^{14}CO_2$ detection with both high selectivity and high sensitivity. In this work, we propose a double-resonance quantitative measurement method, obtain the absorption coefficient of the target molecule in the stepped double-resonance spectroscopy theoretically, and simulate the double-resonance absorption spectra of $^{14}CO_2$. The results show that this scheme can achieve high-selectivity detection of $^{14}CO_2$ at the sub-ppt level.

II. METHOD

The double-resonance method has been widely used in the study of molecular excited states, dynamics and precision spectroscopy [22–24]. The principle of the stepped double-resonance spectroscopy method based on a single-frequency laser that we use is shown in FIG. 1(a). The double-resonance method is based on the pump-probe measurement between three energy levels of a molecule. The pump laser transfers molecules from the E_1 state to the E_2 state, and the probe laser uses the transition from the E_2 state to the E_3 state to measure the molecular population on the E_2 state. If the lifetime of the E_2 state is sufficiently long and the relaxation rate is slow (ro-vibration states of most molecules meet this requirement), molecules in the E_2

DOI:10.1063/1674-0068/cjcp2103045

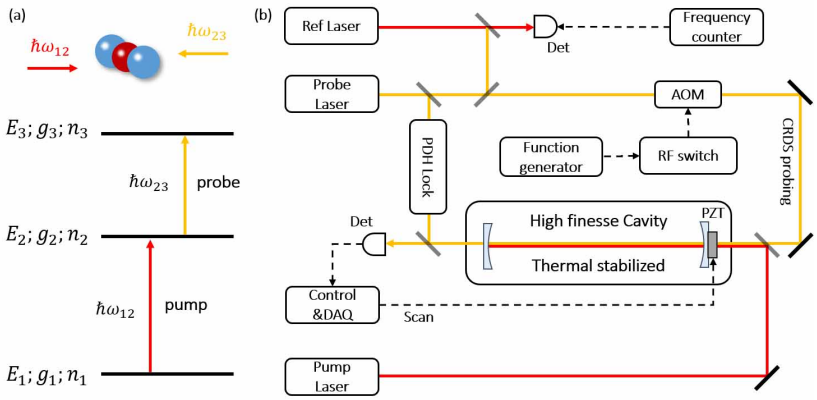

FIG. 1 Schematic of double-resonance spectroscopy. (a) Three-level scheme of the molecule interacting with two lasers and the lasers are resonant with molecules with a velocity of V_z. ω_{12} and ω_{23} denote the frequencies of the pump laser and the probe laser, respectively. The three energy levels are denoted as E_1, E_2 and E_3, the number densitiy of the selected molecules in the three energy levels are n_1, n_2, and n_3, and the degeneracies in the three energy levels are g_1, g_2 and g_3. (b) Configuration of the experiment setup. Det: detector, AOM: acousto-optical modulator, PZT: piezoelectric actuator, DAQ: data acquisition system, Ref: reference.

state can be detected by the probe laser. Since the double-resonance process eliminates the Doppler broadening, the linewidth of the transition can be very narrow. By selecting the appropriate double-resonance transition, the interference of other molecular transitions can be reduced, and the selective detection of specific isotopes can be achieved.

The double-resonance spectroscopy apparatus we are building for the quantitative measurement of $^{14}CO_2$ is shown in FIG. 1(b). A high-finesse optical cavity is composed of a pair of high-reflectivity (HR, R=99.996%) mirrors and an Invar spacer. One of the HR mirrors is attached to a piezoelectric actuator (PZT) for fine tuning of the cavity length. The length of the optical cavity is about 60 cm, and the free spectral range (FSR) is 250 MHz. According to the reflectivity of the HR mirrors, we can get that the fineness of the optical cavity is 78000 and the mode width of the cavity is 3 kHz. The optical cavity is placed in a vacuum sample chamber and the temperature drift of the cavity is kept less than 5×10^{-3} K through a heating wire and feedback control, so that the fractional change of the optical cavity mode frequency is less than 10^{-8} per hour.

Two home-made optical parametric oscillators (OPO) are used as the light sources of the pump laser and the probe laser, and the principle and configuration of OPO are presented in our previous work [18, 25]. The pump and probe laser beams are collinear in the optical cavity and tuned to near the molecular transition frequencies of the pump laser and the probe laser, respectively. The probe laser is locked on the optical cavity using the PDH method. In addition, the rest laser beam is divided into two paths, one is used to calibrate the laser frequency, and the other is frequency-shifted by an acousto-optic modulator (AOM) and coupled into the optical cavity to perform CRDS measurement. AOM is not only used as a frequency shifter, but also as an optical switch in the CRDS measurement. Details of the laser frequency locking and CRDS detection have been presented in the previous work of our group [26] and the mode match of the double-resonance spectroscopy is described in our another work [24]. In this work, the power of the pump laser needs to be as large as possible to obtain sufficient E_2 state population, while the probe laser only needs a few milliwatts for CRDS detection without significant change in the population on the E_2 state.

Since there is rare commercial optical frequency comb in the mid-infrared band, it is difficult to lock the optical cavity to an optical comb as used in our previous work [24]. The scanning of the double-resonance spectroscopy proposed in this work can be accomplished by directly scanning the cavity length of the optical cavity, as shown in FIG. 1(b). During the scanning, we measure the beat frequency between the probe laser and another frequency-stabilized reference laser. The reference laser is a mid-infrared laser whose frequency is locked on an ultra-stable optical cavity [27, 28]. After locking to the ultra-stable optical cavity, the frequency

DOI:10.1063/1674-0068/cjcp2103045

drift of the reference laser has been measured to be less than 0.5 Hz/s, and the long-term stability is better than 10^{-11}. With this method, the frequency accuracy could be better than 10 kHz, which is good enough for the quantitative detection of $^{14}CO_2$.

We assume that the probe laser does not change the molecular population on the energy levels, and the molecular population on the E_2 state and E_3 state can be ignored under equilibrium conditions when the pump laser is off. In the double-resonance process, when the pump laser is on, molecules with the axial velocity V_z at the E_1 state will be transferred to the E_2 state. The relative proportion of molecules populated at the E_2 state is determined by the saturation parameter s and the selected specific speed V_z:

$$\frac{n_2}{N} = \frac{s}{1+2s} I_A \frac{1}{Q(T)} g_1 \mathrm{e}^{-\frac{E_1}{k_\mathrm{B}T}} \frac{1}{V_\mathrm{p}\sqrt{\pi}} \mathrm{e}^{-\frac{{V_z}^2}{{V_p}^2}} \delta V_z \quad (1)$$

where N is the number density of all the CO_2 molecules, n_2 is the number density of the target molecules populated in the E_2 state, I_A is the isotopic abundance, $Q(T)$ is the partition function at temperature T, and V_p is the most probable velocity. Known that for the vibrational transition, the relaxation rate of both the E_1 state and the E_2 state are much smaller than the Rabi frequency of the transition. The saturation parameter s is defined as s=$I_\mathrm{pump}/I_{\mathrm{s}_{12}}$, where I_pump is the power density of the pump laser, and $I_{\mathrm{s}_{12}}$ is the saturation power density of the transition between the E_1 state and the E_2 state, which could be derived according to the following formula [29]:

$$I_{\mathrm{s}_{12}} = \frac{16\pi^4 c\hbar\nu_{12}^3\Gamma^2}{3A_{21}} \quad (2)$$

where c is the speed of light, $\hbar$ is the Planck constant, A_{21} is the Einstein A coefficient, ν_{12} is the transition frequency from the E_1 state to the E_2 state, and Γ is the full width at half maximum (FWHM) of the transition. The linewidth of a molecular ro-vibrational transition in the double-resonance process mainly consists of the transit-time broadening linewidth Γ_t and the collision-induced broadening linewidth:

$$\Gamma = \Gamma_t + \gamma p \quad (3)$$

where p is the sample pressure, and γ is the pressure-broadening coefficient.

The principle of the double-resonance method for quantitative detection is essentially the same as that of conventional laser absorption spectroscopy technologies which are based on Lambert-Beer's law. By measuring the molecular absorption signal on a given path, the absorption coefficient α of the target molecule is obtained. In the double-resonance measurement, the molecule will be transferred from the E_2 state to the E_3 state by the probe laser. According to the law of light absorption and the Einstein relationship of stimulated two-state resonant absorption, we can get:

$$\alpha(\nu)\delta\nu = \frac{\hbar\nu_{23}}{c}(B_{23}n_2 - B_{32}n_3) \quad (4)$$

where ν_{23} is the transition frequency from the E_2 state to the E_3 state. Considering the relationship between the Doppler shift and the molecular velocity, ν_V=$\nu_{23}(1 + V_z/c)$, the relationship between Einstein's A and B coefficients, and assuming that n_2 is only generated by pump laser excitation and n_3 could be neglected, we can obtain the absorption coefficient at the center of the double-resonance spectrum:

$$\alpha(\nu_V) = \frac{A_{32}}{8\pi\nu_{23}^2}\frac{g_3}{g_2} N \frac{s}{1+2s} I_A \frac{g_1 \mathrm{e}^{-\frac{E_1}{k_\mathrm{B}T}}}{Q(T)} \frac{1}{V_\mathrm{p}\sqrt{\pi}} \mathrm{e}^{-\frac{{V_z}^2}{{V_p}^2}} \quad (5)$$

In double-resonance measurement, the obtained spectrum is Doppler-free since the two lasers interact with molecules of a specific velocity at the same time. When the laser linewidth is much narrower than the Doppler width, the velocity distribution of excited molecules could be ignored. Therefore, only the transit-time broadening and collisional broadening need to be considered, and the Lorentzian function could be used to model the line profile.

It can be seen from the equations above that the double-resonance method can quantitatively detect the molecular concentration when the following conditions are met: (i) The pump laser makes the transition from the E_1 state to the E_2 state saturated, or maintains a stable level, to ensure that $s/(1+2s)$ is constant. (ii) The probe laser that detects the transition from the E_2 state to the E_3 state is weak, without affecting the transition from the E_1 state to the E_2 state. Compared with the traditional absorption spectroscopy, double-resonance spectroscopy has a narrower linewidth, and the resolution is consequently improved. The narrower linewidth is less susceptible to the effect of detection noise, such as the optical interference fringes in con-

DOI:10.1063/1674-0068/cjcp2103045

TABLE I The concentration of each molecule in the CO_2 sample.

$^{12}CO_2$	$^{13}CO_2$	$^{16}O^{12}C^{18}O$	$^{16}O^{12}C^{17}O$	$^{16}O^{13}C^{18}O$	$^{16}O^{13}C^{17}O$	$^{14}CO_2$	$^{14}N_2^{16}O$
0.984204	0.011057	0.003947	7.339890×10^{-4}	4.434460×10^{-5}	8.246320×10^{-6}	1.176×10^{-12}	1×10^{-9}

ventional CRDS measurements [30], and the sensitivity of detection is further improved. In addition, it avoids the nonlinear effect in the saturated absorption spectroscopy, which leads to a deterioration of the quantitative measurement.

III. RESULTS AND DISCUSSION

Since there are fewer interfering features near the P(20) transition line of the fundamental band (00011−00001) of $^{14}CO_2$, the (00011−00001) P(20) line of $^{14}CO_2$ near 4.5 μm is currently the most widely used transition for single-photon spectroscopy detection of $^{14}CO_2$ [2]. FIG. 2 is the simulated single-photon absorption spectra of the CO_2 sample near the (00011−00001) P(20) transition line of $^{14}CO_2$. All molecular concentrations in the CO_2 sample we used are shown in Table I. The natural abundance [31] of each isotopologue of carbon dioxide is used in the simulation. Given that there may be the absorption of nitrogen oxides in the sample, its concentration is set to 10^{-9} according to the experimental results of the Fleisher group [20].

According to the experimental conditions given in Ref.[20], we used a sample pressure of 0.9 kPa in the simulation. The temperatures in FIG. 2 are 296 K, 220 K and 170 K, respectively. The Voigt line profile is used in the simulation. The black solid line in FIG. 2 is the simulated spectrum that contains all molecular transitions in the CO_2 sample shown in Table I. For comparison, we use lines with different colors to represent different molecules. It can be seen from the simulation that the single-photon absorption method cannot distinguish $^{14}CO_2$ at the room temperature. As the temperature of the CO_2 sample decreases, the Doppler linewidth of each CO_2 isotope gradually narrows. However, the width (FWHM) of the transition is still about 200 MHz at 220 K. At this temperature, the absorption spectrum of $^{14}CO_2$ can be distinguished from the nearby spectra of $^{13}CO_2$ and N_2O, but the quantitative measurement of $^{14}CO_2$ is still a big challenge due to the low concentration of $^{14}CO_2$. It is worth noting that the interfering lines of $^{13}CO_2$ are in the hot bands (05511−05501) P(13)e and (21111−21101) P(19)e [31],

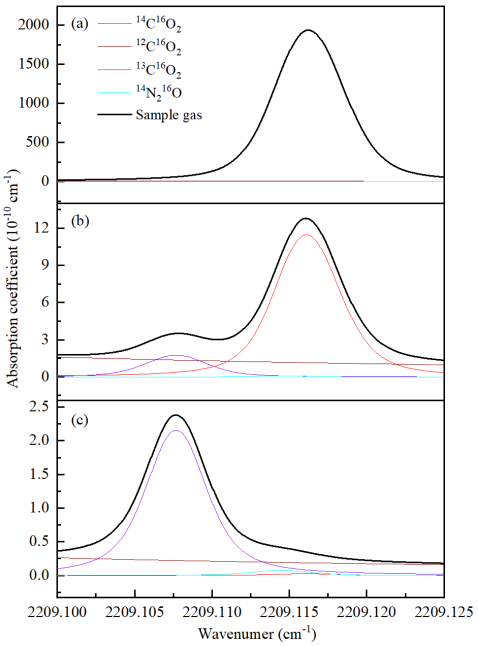

FIG. 2 Comparison of single-photon absorption spectra at different temperatures under 900 Pa sample pressure. The purple, brown, red, cyan and black solid lines represent the spectra of $^{14}C^{16}O_2$, $^{12}C^{16}O_2$, $^{13}C^{16}O_2$, $^{14}N_2{}^{16}O$ and sample gas, respectively. (a) T=296 K, (b) T=220 K, (c) T=170 K.

which will be further reduced as the temperature decreases. As shown in FIG. 2(c), detection under lower temperature can significantly reduce the signal of interfering transition lines although it increases the complexity of the experiment. Note that the concentration of N_2O used in this simulation is 1 ppb and the average concentration of N_2O in the atmosphere is 324.2 ppb [32], which is about 0.1% of CO_2, known as 390.5 ppm [32]. To reduce the N_2O concentration to 1 ppb of the CO_2 sample, complex physical and chemical methods must be applied to pretreat the sample.

FIG. 3 shows the simulated double-resonance absorption spectrum of the CO_2 sample at 250 K. The pump laser is resonant with the (00011−00001) R(16) transition of $^{14}CO_2$ near 4468 nm, and the probe laser is resonant with the (00021−00011) P(17) transition of $^{14}CO_2$ near 4567 nm. The pump laser power density we used in the simulation is 3.25×10^7 W/m^2, which is easy to realize in the cavity-locked CRDS [26]. The sample pressure is set to 900 Pa, which is the same

DOI:10.1063/1674-0068/cjcp2103045

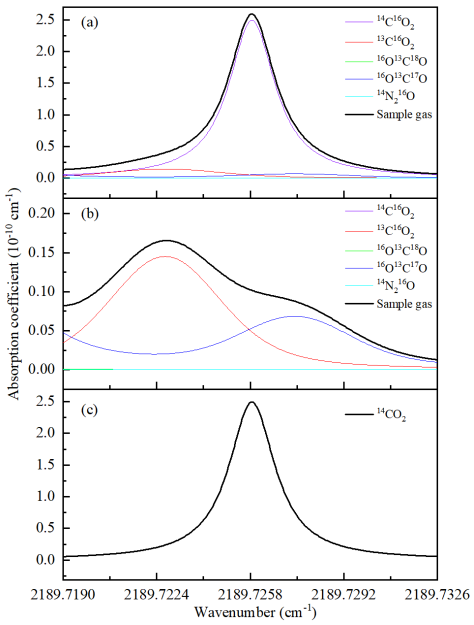

FIG. 3 Simulated double-resonance absorption spectrum of the CO_2 sample at 250 K and 900 Pa. γ=0.23 cm^{-1} atm^{-1} [33]. (a) Absorption spectra of the CO_2 sample and its different components when the pump laser is turned on. (b) Absorption spectra of the CO_2 sample (the background) and its different components when the pump laser is turned off. The purple, red, green, blue, cyan and black solid lines in (a) and (b) represent the spectrum of $^{14}C^{16}O_2$, $^{13}C^{16}O_2$, $^{16}O^{13}C^{18}O$, $^{16}O^{13}C^{17}O$, $^{14}N_2^{16}O$ and sample gas, respectively. (c) The absorption spectrum of $^{14}CO_2$ after the absorption spectra of other molecules removed by the differential method.

as the pressure we used in the simulation of single-photon spectroscopy. The Doppler-free peak recorded by the double-resonance method has a considerable narrow linewidth, the value of which is limited by the collision-induced broadening and transit-time broadening. As shown in FIG. 3, the double-resonance spectrum of $^{14}CO_2$ at 250 K is only slightly overlapped with interfering transitions from other CO_2 isotopologues. Furthermore, since the pump and the probe lasers are from two independent light sources, we are able to measure the spectra of interfering molecules directly (shown in FIG. 3(b)) in the experiment by turning off the pump laser, and use a differential method to eliminate the effect of the absorption of interfering molecules in the CO_2 sample, which can greatly improve the accuracy of quantitative analysis. It is worth noting that even higher concentration of N_2O is presented in the sample, the differential double-resonance spectroscopy can effectively eliminate the interference due to N_2O, which greatly simplifies the procedure of sample pretreatment.

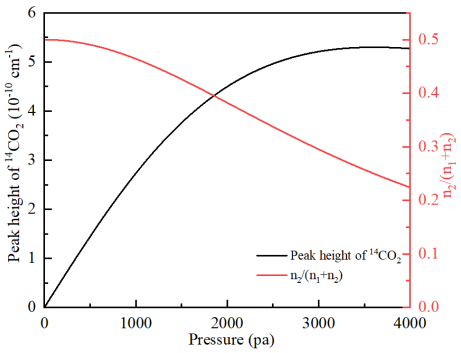

FIG. 4 Under different sample pressures, the double-resonance peak height of $^{14}CO_2$ spectrum (black solid line) and the population ratio $n_2/(n_1+n_2)$ (red solid line) of molecules populated in the E_2 state.

FIG. 4 shows the simulated peak height of the $^{14}CO_2$ double-resonance spectrum and the proportion of the population on the E_2 state at different sample pressures at 250 K. The pump laser power density was set at 3.25×10^7 W/m^2 in the simulation. The population ratio $n_2/(n_1+n_2)$ of the molecules with the selected velocity V_z on the E_2 state equalls to $s/(1+2s)$. When the pump laser power is fixed, the peak height of the double-resonance spectrum increases rapidly with the sample pressure below 2000 Pa since the molecular number density increases linearly with the sample pressure. When the sample pressure increases sequentially, the growth rate of the peak height is reduced since there is less and less molecular population on the E_2 state, as the red solid line in FIG. 4 shows. The line width of the double-resonance spectrum keeps increasing linearly with the pressure, which will affect the resolution of the double-resonance measurement. In practical measurement, $^{14}CO_2$ concentration can be measured under fixed sample pressure below 2000 Pa where the signal-to-noise ratio is good enough and the linewidth is still narrow. In our previous work, we have achieved a sensitivity of 6×10^{-11} cm^{-1} (average time 30 min) by using the CRDS method in the mid-infrared region [18]. It is expected that the measurement of $^{14}CO_2$ with an abundance of 0.24 ppt can be achieved in half an hour under pressure of 1 kPa at 250 K. And the detection sensitivity can be further improved if the laser is locked with the optical cavity [19, 34].

As the CRDS technology is more mature in the near-infrared region, we can use near-infrared laser as the probe laser and mid-infrared laser as the pump laser to perform double resonance spectroscopy, aiming at quantitative measurement of enriched samples. The experi-

DOI:10.1063/1674-0068/cjcp2103045

mental scheme is similar to the configuration described in FIG. 1. The HR mirrors are coated with a two-color film as used in our previous work [24], which has characteristics of low-loss and high-reflectivity for both the pump and probe lasers. Compared with the setup in FIG. 1, it is easier to control and record the probe laser frequency, resulting in a better spectroscopy frequency accuracy. Moreover, the detection sensitivity of CRDS in the near-infrared region has already reached 1×10^{-12} cm^{-1} [34]. We choose a laser at 4470 nm near the (00011−00001) R(14) transition line as the pump laser and a laser at 1525 nm near the (00041−00011) R(15) transition line as the probe laser to demonstrate the double-resonance detection of $^{14}CO_2$-enriched sample. Note that the transitions in the (00041−00011) band are usually weaker by 3−4 orders of magnitude than the fundamental band, so we use $^{14}CO_2$ with the concentration of 1×10^{-8} in the simulation and the results are shown in FIG. 5. There is less absorption lines of other CO_2 isotopologues near the (00041−00011) R(15) line of $^{14}CO_2$ due to the larger isotopic shift of overtone transitions. The interfering molecules here only raised the baseline, as shown in FIG. 5(a). Given that the big difference between the frequency of the pump laser and the probe laser, it is easier to modulate the mid-infrared pump laser to remove the background. The modulated differential double-resonance spectrum will not be affected by the baseline, as shown in FIG. 5(c). For some applications that the concentration of $^{14}CO_2$ in the sample is enriched, such as biomedical studies and radioactive pollution monitoring, the near-infrared-mid-infrared double-resonance spectroscopy method could significantly reduce the cost and improve the compatibility of the instrument.

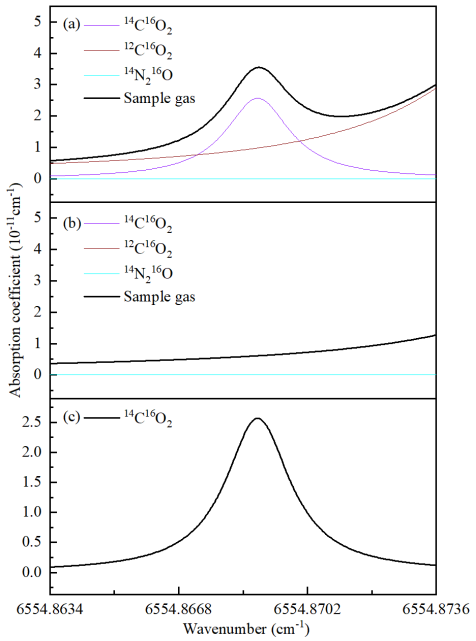

FIG. 5 Simulated double-resonance absorption spectrum of the CO_2 sample at 250 K and 900 Pa by using a mid-infrared laser as a pump laser and a near-infrared laser as a probe laser. γ=0.234 $cm^{-1}atm^{-1}$ [33]. The purple, brown, cyan and black solid lines represent the spectrum of $^{14}C^{16}O_2$, $^{12}C^{16}O_2$, $^{14}N_2{}^{16}O$ and sample gas, respectively. (a) Absorption spectra of the CO_2 sample and its different components when the pump laser is turned on. (b) Absorption spectra of the CO_2 sample (the background) and its different components when the pump laser is turned off. (c) The absorption spectrum of $^{14}CO_2$ after the background removed by differential method.

IV. CONCLUSION

In this work, a stepped double-resonance absorption spectroscopy method which can realize high-resolution Doppler-free spectral detection is proposed to achieve selective detection of $^{14}CO_2$. And the accuracy of quantitative measurement can be further improved by modulating the pump laser to eliminate the background consisting of the absorption spectra of other molecules except for $^{14}CO_2$ in the sample. Using the highly sensitive CRDS technology, $^{14}CO_2$ measurement with high selectivity and a sensitivity of sub-ppt level can be achieved. Finally, it is worth pointing out that the double-resonance absorption spectroscopy method proposed in this work is not limited to the quantitative measurement of $^{14}CO_2$. As long as the appropriate molecular transitions are selected, this method is also suitable for selective detection of other molecular isotopologues. The background-free double-resonance spectroscopy method is expected to further promote the application of laser spectroscopy in trace detection of molecules, including environmental science, biomedicine, and earth science.

V. ACKNOWLEDGMENTS

This work was jointly supported by the National Natural Science Foundation of China (No.21688102, No.11974328), the Chinese Academy of Sciences (XDB21020100, XDC07010000), and Anhui Initiative in Quantum Information Technologies (AHY110000).

[1] W. G. Mook and J. Van Der Plicht, Radiocarbon **41**, 227 (1999).

[2] A. Maity, S. Maithani, and M. Pradhan, Anal. Chem. **93**, 388 (2020).
[3] J. R. Arnold and W. F. Libby, Science **113**, 111 (1951).
[4] I. Levin and V. Hesshaimer, Radiocarbon **42**, 69 (2000).
[5] S. Hammer, R. Friedrich, B. Kromer, A. Cherkinsky, S. Lehman, and H. Meijer, Radiocarbon **59**, 875 (2017).
[6] L. Wacker, G. Bonani, M. Friedrich, I. Hajdas, B. Kromer, M. Němec, M. Ruff, M. Suter, H. A. Synal, and C. Vockenhuber, Radiocarbon **52**, 252 (2010).
[7] N. A. Kratochwil, S. R. Dueker, D. Muri, C. Senn, H. Yoon, B. Y. Yu, G. H. Lee, F. Dong, and M. B. Otteneder, PLoS One **13**, 0205435 (2018).
[8] C. B. Ramsey, C. Brenninkmeijer, P. Jöckel, H. Kjeldsen, and J. Masarik, Nucl. Instrum. Meth. B. **259**, 558 (2007).
[9] C. A. Brenninkmeijer, M. R. Manning, D. C. Lowe, G. Wallace, R. J. Sparks, and A. Volz Thomas, Nature **356**, 50 (1992).
[10] J. Moriizumi, A. Goto, and T. Iida, Nucl. Instrum. Meth. B **223**, 511 (2004).
[11] S. Schilt, L. Thévenaz, M. Niklès, L. Emmenegger, and C. Hüglin, Spectrochim. Acta A **60**, 3259 (2004).
[12] T. Tomberg, M. Vainio, T. Hieta, and L. Halonen, Sci. Rep. **8**, 1 (2018).
[13] D. Labrie and J. Reid, Appl. Phys. A **24**, 381 (1981).
[14] A. Kosterev, G. Wysocki, Y. Bakhirkin, S. So, R. Lewicki, M. Fraser, F. Tittel, and R. Curl, Appl. Phys. B **90**, 165 (2008).
[15] Y. Yao, A. J. Hoffman, and C. F. Gmachl, Nat. Photonics. **6**, 432 (2012).
[16] I. Ventrillard, P. Gorrotxategi Carbajo, and D. Romanini, Appl. Phys. B **123**, 1 (2017).
[17] S. Borri, G. Insero, G. Santambrogio, D. Mazzotti, F. Cappelli, I. Galli, G. Galzerano, M. Marangoni, P. Laporta, V. Di Sarno, L. Santamaria, P. Maddaloni, and P. De Natale, Appl. Phys. B **125**, 18 (2019).
[18] Z. T. Zhang, C. F. Cheng, Y. R. Sun, A. W. Liu, and S. M. Hu, Opt. Express **28**, 27600 (2020).
[19] I. Galli, S. Bartalini, R. Ballerini, M. Barucci, P. Cancio, M. De Pas, G. Giusfredi, D. Mazzotti, N. Akikusa, and P. De Natale, Optica **3**, 385 (2016).
[20] A. J. Fleisher, D. A. Long, Q. Liu, L. Gameson, and J. T. Hodges, J. Phys. Chem. Lett. **8**, 4550 (2017).
[21] R. M. Wilson, Phys. Today **69** (2016).
[22] A. Callegari, H. Srivastava, U. Merker, K. Lehmann, G. Scoles, and M. Davis, J. Chem. Phys. **106**, 432 (1997).
[23] C. H. Zhang and G. H. Sha, Science **262**, 374 (1993).
[24] C. L. Hu, V. I. Perevalov, C. F. Cheng, T. P. Hua, A. W. Liu, Y. R. Sun, Y. Tan, J. Wang, and S. M. Hu, J. Phys. Chem. Lett. **11**, 7843 (2020).
[25] Z. T. Zhang, Y. Tan, J. Wang, C. F. Cheng, Y. R. Sun, A. W. Liu, and S. M. Hu, Opt. Lett. **45**, 1013 (2020).
[26] L. G. Tao, A. W. Liu, K. Pachucki, J. Komasa, Y. R. Sun, J. Wang, and S. M. Hu, Phys. Rev. Lett. **120**, 153001 (2018).
[27] M. S. Taubman, T. L. Myers, B. D. Cannon, R. M. Williams, F. Capasso, C. Gmachl, D. L. Sivco, and A. Y. Cho, Opt. Lett. **27**, 2164 (2002).
[28] M. S. Taubman, T. L. Myers, B. D. Cannon, and R. M. Williams, Spectrochim. Acta. A **60**, 3457 (2004).
[29] G. Giusfredi, S. Bartalini, S. Borri, P. Cancio, I. Galli, D. Mazzotti, and P. De Natale, Phys. Rev. Lett. **104**, 110801 (2010).
[30] J. Burkart and S. Kassi, Appl. Phys. B **119**, 97 (2015).
[31] I. E. Gordon, L. S. Rothman, C. Hill, R. V. Kochanov, Y. Tan, P. F. Bernath, M. Birk, V. Boudon, A. Campargue, K. Chance, B. J. Drouin, J. M. Flaud, R. R. Gamache, J. T. Hodges, D. Jacquemart, V. I. Perevalov, A. Perrin, K. P. Shine, M. A. Smith, J. Tennyson, G. C. Toon, H. Tran, V. G. Tyuterev, A. Barbe, A. G. Csszr, V. M. Devi, T. Furtenbacher, J. J. Harrison, J. M. Hartmann, A. Jolly, T. J. Johnson, T. Karman, I. Kleiner, A. A. Kyuberis, J. Loos, O. M. Lyulin, S. T. Massie, S. N. Mikhailenko, N. Moazzen Ahmadi, H. S. Mller, O. V. Naumenko, A. V. Nikitin, O. L. Polyansky, M. Rey, M. Rotger, S. W. Sharpe, K. Sung, E. Starikova, S. A. Tashkun, J. V. Auwera, G. Wagner, J. Wilzewski, P. Wciso, S. Yu, and E. J. Zak, J. Quant. Spectrosc. Radiat. **203**, 3 (2017).
[32] D. L. Hartmann, A. M. K. Tank, M. Rusticucci, L. V. Alexander, S. Brönnimann, Y. A. R. Charabi, F. J. Dentener, E. J. Dlugokencky, D. R. Easterling, A. Kaplan, J. S. Brian, W. T. Peter, W. Martin, and Z. Panmao, in *Climate Change 2013 the Physical Science Basis: Working Group I contribution to the fifth Assessment Report of the Intergovernmental Panel on Climate Change,* Cambridge University Press, 159, (2013).
[33] L. S. Rothman, I. E. Gordon, Y. Babikov, A. Barbe, D. C. Benner, P. F. Bernath, M. Birk, L. Bizzocchi, V. Boudon, L. R. Brown, A. Campargue, K. Chance, E. A. Cohen, L. H. Coudert, V. M. Devi, B. J. Drouin, A. Fayt, J. M. Flaud, R. R. Gamache, J. J. Harrison, J. M. Hartmann, C. Hill, J. T. Hodges, D. Jacquemart, A. Jolly, J. Lamouroux, R. J. Le Roy, G. Li, D. A. Long, O. M. Lyulin, C. J. Mackie, S. T. Massie, S. Mikhailenko, H. S. Mller, O. V. Naumenko, A. V. Nikitin, J. Orphal, V. Perevalov, A. Perrin, E. R. Polovtseva, C. Richard, M. A. Smith, E. Starikova, K. Sung, S. Tashkun, J. Tennyson, G. C. Toon, V. G. Tyuterev, and G. Wagner, J. Quant. Spectrosc. Radiat. **130**, 4 (2013).
[34] J. Wang, Y. R. Sun, L. G. Tao, A. W. Liu, and S. M. Hu, J. Chem. Phys. **147**, 091103 (2017).

DOI:10.1063/1674-0068/cjcp2103045